

# Solid-State Coordination Chemistry of Molybdenum Oxides with di-2-Picolylamine (pca): The Hydrothermal Syntheses and Structures of the Molecular Cluster $[\{\text{Ni}(\text{pca})(\text{H}_2\text{O})\}_2\text{Mo}_8\text{O}_{26}]$ , the Two-Dimensional $[\{\text{Cu}(\text{pca})\}_2\text{Mo}_8\text{O}_{26}]$ , and the One-Dimensional $[\{\text{Cu}_3(\text{pca})_3\text{MoO}_4\}\text{Mo}_8\text{O}_{26}]$

Randy S. Rarig, Jr. and Jon Zubieta<sup>1</sup>

Department of Chemistry, Syracuse University, Syracuse, New York 13244

Received October 29, 2001; accepted February 22, 2002

IN HONOR OF PROFESSOR GALEN STUCKY ON THE OCCASION OF HIS 65TH BIRTHDAY

The hydrothermal reaction of di-2-picolylamine (pca),  $\text{MoO}_3$  and  $\text{NiSO}_4 \cdot 6\text{H}_2\text{O}$  yielded the bimetallic oxide cluster  $[\{\text{Ni}(\text{pca})(\text{H}_2\text{O})\}_2\text{Mo}_8\text{O}_{26}] \cdot 2\text{H}_2\text{O}$  ( $1 \cdot 2\text{H}_2\text{O}$ ). Similarly, the reaction of pca,  $\text{MoO}_3$  and  $\text{CuSO}_4 \cdot 5\text{H}_2\text{O}$  produced the two-dimensional material  $[\{\text{Cu}(\text{pca})\}_2\text{Mo}_8\text{O}_{26}]$  (2). The structure of 1 consists of  $\beta$ - $\{\text{Mo}_8\text{O}_{26}\}^{4-}$  clusters, decorated with  $\{\text{Ni}(\text{pca})(\text{H}_2\text{O})\}^{2+}$  subunits, linked to terminal molybdenyl  $\{\text{Mo}=\text{O}\}$  moieties. The structure of 2 also contains  $\beta$ - $\{\text{Mo}_8\text{O}_{26}\}^{4-}$  clusters as building blocks; however, in this instance, the  $\{\text{Cu}(\text{pca})\}^{2+}$  subunits serve to bridge adjacent clusters into a two-dimensional network. The hydrothermal reaction of pca and  $\text{CuSO}_4 \cdot 5\text{H}_2\text{O}$  with  $\text{MoO}_2$  in place of  $\text{MoO}_3$  produced  $[\{\text{Cu}_3(\text{pca})_3\text{MoO}_4\}\text{Mo}_8\text{O}_{26}] \cdot 2\text{H}_2\text{O}$  ( $3 \cdot 2\text{H}_2\text{O}$ ), a one-dimensional material, constructed from  $\beta$ - $\{\text{Mo}_8\text{O}_{26}\}^{4-}$  clusters linked through unusual  $\{\text{Cu}_3(\text{pca})_3\text{MoO}_4\}^{4+}$  subunits. Crystal data:  $\text{C}_{12}\text{H}_{17}\text{N}_3\text{O}_{15}\text{Mo}_4\text{Ni}$  ( $1 \cdot 2\text{H}_2\text{O}$ ): triclinic  $P\bar{1}$ ,  $a = 9.4024(5) \text{ \AA}$ ,  $b = 10.9729(6) \text{ \AA}$ ,  $c = 11.4183(6) \text{ \AA}$ ,  $\alpha = 102.710(1)^\circ$ ,  $\beta = 99.731(1)^\circ$ ,  $\gamma = 90.021(1)^\circ$ ,  $V = 1131.8(1) \text{ \AA}^3$ ,  $Z = 2$ ,  $D_{\text{calc}} = 2.596 \text{ g cm}^{-3}$ ;  $\text{C}_{12}\text{H}_{13}\text{N}_3\text{O}_{13}\text{Mo}_4\text{Cu}$  (2): monoclinic  $P2_1/n$ ,  $a = 12.1547(4) \text{ \AA}$ ,  $b = 12.5412(4) \text{ \AA}$ ,  $c = 14.1160(4) \text{ \AA}$ ,  $\beta = 92.746(1)^\circ$ ,  $V = 2149.3(1) \text{ \AA}^3$ ,  $Z = 4$ ,  $D_{\text{calc}} = 2.638 \text{ g cm}^{-3}$ ;  $\text{C}_{36}\text{H}_{43}\text{Cu}_3\text{Mo}_9\text{N}_9\text{O}_{32}$  ( $3 \cdot 2\text{H}_2\text{O}$ ), monoclinic,  $P2_1/c$ ,  $a = 17.9115(6) \text{ \AA}$ ,  $b = 14.3637(5) \text{ \AA}$ ,  $c = 22.6795(8) \text{ \AA}$ ,  $\beta = 94.744(1)^\circ$ ,  $V = 5814.9(3) \text{ \AA}^3$ ,  $Z = 4$ ,  $D_{\text{calc}} = 2.476 \text{ g cm}^{-3}$ . © 2002 Elsevier Science (USA)

**Key Words:** molybdenum oxides; hydrothermal synthesis; organic–inorganic hybrid materials; oxide clusters.

## INTRODUCTION

Hybrid materials combine the unique characteristics of organic and inorganic components to provide new solid-state architectures with composite or novel properties (1).

<sup>1</sup>To whom correspondence should be addressed. E-mail: jazubiet@syr.edu.

Examples include inorganic oxide materials, such as zeolites (2), mesoporous compounds of the MCM-41 class (3), and organically templated transition metal phosphates (4), as well as organic–inorganic halides of the perovskite family (5).

Our approach to the design of novel oxovanadium- and oxomolybdenum-based materials relies on the principles of fundamental coordination chemistry to modify the oxide microstructure (6, 7). The organic component is introduced as a ligand to a secondary metal site, which functions as an integral subunit of the covalent architecture of the solid. The overall structure of the hybrid reflects the coordination preferences of the secondary metal site, as well as the geometric and coordination constraints of the ligand. In the case of molybdenum oxide materials, the well-developed polyoxoanion chemistry provides a variety of cluster buildings which may be exploited in a “tinker toy” design approach (8).

Ligand denticity is an obvious characteristic which can be varied in such syntheses. The consequences of different ligand denticities are apparent in the structures of the series of materials  $[\{M'(2,2'\text{-bpy})_n\}\text{Mo}_x\text{O}_y]$  (9) and  $[\{M'(\text{terpy})\}\text{Mo}_x\text{O}_y]$  (10), as well as  $[\{\text{Cu}(2,2'\text{-bpy})_n\}\text{V}_x\text{O}_y(\text{H}_m\text{PO}_4)_z]$  and  $[\{\text{Cu}(\text{terpy})\}_2\text{V}_x\text{O}_y(\text{H}_n\text{PO}_4)_z]$  (11). In this contribution, the structural influences of the tridentate ligand di-2-picolylamine are investigated with the  $M'/\text{Mo}/\text{O}$  family. The syntheses and structures of  $[\{\text{Ni}(\text{pca})(\text{H}_2\text{O})\}_2\text{Mo}_8\text{O}_{26}] \cdot \text{H}_2\text{O}$  ( $1 \cdot \text{H}_2\text{O}$ ) and  $[\{\text{Cu}(\text{pca})\}_2\text{Mo}_8\text{O}_{26}]$  as well as the behavior of the system with  $M' = \text{Mn}(\text{II})$ ,  $\text{Fe}(\text{II})$ ,  $\text{Co}(\text{II})$ , and  $\text{Zn}(\text{II})$  are described.

## EXPERIMENTAL SECTION

Reagents were purchased from Aldrich Chemical Co. and used without further purification. All syntheses were



carried out in 23 mL polytetrafluoroethylene-lined Parr stainless-steel containers or borosilicate tubes under auto-genous pressure. The reactants were stirred briefly before heating. Water was distilled above 3.0 M $\Omega$  in-house using a Barnstead Model 525 Biopure Distilled Water Center.

*Synthesis of*  $[\{[Ni(pca)(H_2O)]_2Mo_8O_{26}\} \cdot 2H_2O (1 \cdot 2H_2O)]$ . A mixture of  $NiSO_4 \cdot 6H_2O$  (0.084 g, 0.32 mmol),  $MoO_3$  (0.036 g, 0.25 mmol), di-2-picolyamine (0.033 g, 0.16 mmol) and  $H_2O$  (5.76 g, 320 mmol) was heated at 140°C for 48 h. After cooling, green crystals of  $1 \cdot 2H_2O$  were collected in 60% yield. IR (KBr pellet,  $cm^{-1}$ ): 3296(m), 1655(s), 1570(s), 1505(s), 1290(m), 943(vs), 908(vs), 851(s).

*Synthesis of*  $[\{Cu(pca)\}_2Mo_8O_{26}] (2)$ . A mixture of  $CuSO_4 \cdot 5H_2O$  (0.11 g, 0.44 mmol),  $MoO_3$  (0.048 g, 0.31 mmol), di-2-picolyamine (0.044 g, 0.21 mmol) and  $H_2O$  (9.45 g, 525 mmol) was heated at 120°C for 48 h. After cooling to room temperature, blue crystals of **2** were obtained in 45% yield. IR (KBr pellet,  $cm^{-1}$ ): 3223(m), 1654(s), 1576(s), 1508(s), 1285(n), 959(vs), 913(vs), 843(vs).

*Synthesis of*  $[\{Cu_3(pca)_3MoO_4\}Mo_8O_{26}] \cdot 2H_2O (3 \cdot 2H_2O)$ . A mixture of  $CuSO_4 \cdot 5H_2O$  (0.11 g, 0.44 mmol),  $MoO_2$  (0.043 g, 0.34 mmol), di-2-picolyamine (0.044 g, 0.22 mmol) and  $H_2O$  (9.90 g, 0.55 mol) was heated at 140°C for 48 h. After cooling, blue crystals of  $3 \cdot 2H_2O$  were recovered in 10% yield based on Mo. Attempts to increase the yield by adjusting stoichiometry, changing the reaction temperatures, and modifying the pH of the reaction were unsuccessful.

*Synthesis of*  $[Cu(C_5H_4NCO_2)_2] \cdot 2H_2O (4 \cdot 2H_2O)$ . The synthesis of  $3 \cdot 2H_2O$  was modified by the addition of sufficient  $(C_2H_5)_4NOH$  (40%) to obtain an initial pH of 8.7. All other conditions and reactants were identical to those for the isolation of  $3 \cdot 2H_2O$ . After cooling, blue-green blocks of  $4 \cdot 2H_2O$  were obtained in ca. 20% yield based on molybdenum. Crystal data: triclinic,  $P\bar{1}$ ,  $a = 5.1030(3) \text{ \AA}$ ,  $b = 7.5225(4) \text{ \AA}$ ,  $c = 9.0824(4) \text{ \AA}$ ,  $\alpha = 76.077(1)^\circ$ ,  $\beta = 85.078(1)^\circ$ ,  $\gamma = 72.161(1)^\circ$ ,  $V = 322.11(7) \text{ \AA}^3$ ,  $D_{calc} = 1.772 \text{ g cm}^{-3}$ .

*Synthesis of*  $[Co(C_5H_4NCO_2)_3] \cdot H_2O (5 \cdot H_2O)$ . A mixture of  $Co(NO_3)_2 \cdot 6H_2O$  (0.22 g, 0.76 mmol),  $MoO_3$  (0.10 g, 0.70 mmol), di-2-picolyamine (0.074 g, 0.36 mmol) and  $H_2O$  (9.72 g, 540 mmol) was heated at 180°C for 48 h. After cooling, pink crystals of  $5 \cdot H_2O$  were collected in 55% yield. IR (KBr pellet,  $cm^{-1}$ ): 1618(s), 1555(m), 1500(m), 900(s, br). Crystal data: monoclinic,  $C2/c$ ,  $a = 29.7195(19) \text{ \AA}$ ,  $b = 8.4981(6) \text{ \AA}$ ,  $c = 13.7226(9) \text{ \AA}$ ,  $\beta = 96.218(1)^\circ$ ,  $V = 3445.4(4) \text{ \AA}^3$ ,  $D_{calc} = 1.709 \text{ g cm}^{-3}$ .

### X-Ray Crystallography

Single-crystal diffraction data for **1–3** were measured using a Bruker P4 diffractometer equipped with the

SMART system (12) and using  $MoK\alpha$  radiation ( $\lambda = 0.71073 \text{ \AA}$ ). All data sets were corrected for Lorentz and polarization effects, and absorption corrections were made using SADABS (13). The structure solutions and refinements were carried out using SHELXL96 (14). All structures were solved using direct methods and all of the non-hydrogen atoms were located from the initial solution or from subsequent electron density difference maps during the initial stages of the refinement. After locating all of the non-hydrogen atoms in each structure, the models were refined against  $F^2$ , first using isotropic and finally anisotropic thermal displacement parameters, until the final value of  $\sigma/\Delta_{max}$  was less than 0.001. The positions of the hydrogen atoms were then calculated and fixed, and a final cycle of refinements was performed until  $\sigma/\Delta_{max}$  was again less than 0.001. The crystal data for **1–3** are summarized in Table 1. CCDC reference numbers: 172441–172443. See <http://www.isc.org/?data/dt/b0/> for crystallographic data in CIF format.

## RESULTS AND DISCUSSION

### Syntheses and Infrared Spectra

The compounds of this study were prepared by conventional hydrothermal techniques (15). Thus, the reaction of  $NiSO_4 \cdot 6H_2O$ ,  $MoO_3$ , di-2-picolyamine (pca) and  $H_2O$  in the mole ratio 2:1.5:1:2000 yielded  $[\{Ni(pca)(H_2O)\}_2Mo_8O_{26}] \cdot 2H_2O (1 \cdot 2H_2O)$  in good yield as green crystals. Similarly, the reaction of  $CuSO_4 \cdot 5H_2O$ ,  $MoO_3$ , pca, and  $H_2O$  in the mole ratio 2:1.5:1:2500 provided  $[\{Cu(pca)\}_2Mo_8O_{26}] (2)$  as blue crystals. The influence of reaction conditions on product identity is dramatically illustrated by the isolation of  $[\{Cu_3(pca)_3MoO_4\}Mo_8O_{26}] \cdot 2H_2O (3 \cdot 2H_2O)$ , which is prepared under similar conditions to those employed for **1** and **2** but using  $MoO_2$  in place of  $MoO_3$ . Thus, the reaction of  $CuSO_4 \cdot 5H_2O$ , pca,  $MoO_2$  and water in the mole ratio 2:1:1.5:2500 at 140°C for 48 h yielded  $3 \cdot 2H_2O$  in low yield. These represent the optimized conditions for the syntheses of **1–3**, as changes in stoichiometries, the M(II) salt and pH resulted in poor yields or amorphous mixtures or, in the case of the procedure for  $3 \cdot 2H_2O$ , the previously reported  $[Cu(C_5H_4NCO_2)_2] \cdot 2H_2O (4 \cdot 2H_2O)$  (16). Attempts to prepare analogous materials with Mn(II), Fe(II), Co(II) and Zn(II) under similar conditions in the 120–140°C temperature range yielded only amorphous mixtures. However, upon raising the temperature to 180°C, the reaction of  $Co(NO_3)_2 \cdot 6H_2O$ ,  $MoO_3$ , the pca, and  $H_2O$  in the mole ratio 2.5:2:1:1500 yielded the previously reported  $[Co(C_5H_4NCO_2)_3] \cdot H_2O (5 \cdot H_2O)$  (17). The oxidative cleavage of the pca ligand to produce 2-pyridylcarboxylate and the oxidation of Co(II) to Co(III) in the product are accompanied by reduction of molybdenum (VI) to  $MoO_2$ , the major by-product of the reaction. The analogous

**TABLE 1**  
**Summary of Crystal Data for the Structural Studies of  $[\{\text{Ni}(\text{pca})(\text{H}_2\text{O})\}_2\text{Mo}_8\text{O}_{26}]\cdot 2\text{H}_2\text{O}$  ( $1\cdot 2\text{H}_2\text{O}$ ),  $[\{\text{Cu}(\text{pca})\}_2\text{Mo}_8\text{O}_{26}]$  (**2**) and  $[\{\text{Cu}_3(\text{pca})_3\text{MoO}_4\}_2\text{Mo}_8\text{O}_{26}]\cdot 2\text{H}_2\text{O}$  ( $3\cdot \text{H}_2\text{O}$ )**

	1·2H <sub>2</sub> O	2	3·2H <sub>2</sub> O
Formula	C <sub>12</sub> H <sub>17</sub> N <sub>3</sub> O <sub>15</sub> Mo <sub>4</sub> Ni	C <sub>12</sub> H <sub>13</sub> N <sub>3</sub> O <sub>13</sub> Mo <sub>4</sub> Cu	C <sub>36</sub> H <sub>43</sub> Cu <sub>3</sub> Mo <sub>9</sub> N <sub>9</sub> O <sub>32</sub>
fw	885.75	854.55	2167.87
Space group	<i>P</i> $\bar{1}$	<i>P</i> 2 <sub>1</sub> / <i>n</i>	<i>P</i> 2 <sub>1</sub> / <i>c</i>
<i>a</i> (Å)	9.4024(5)	12.1547(4)	17.9115(6)
<i>b</i> (Å)	10.9729(6)	12.5412(4)	14.3637(5)
<i>c</i> (Å)	11.4183(6)	14.1160(4)	22.6795(8)
$\alpha$ (deg)	102.710(1)	90	90
$\beta$ (deg)	99.731(1)	92.746(1)	94.744(1)
$\gamma$ (deg)	90.021(1)	90	90
<i>V</i> (Å <sup>3</sup> )	1131.8(1)	2149.3(1)	5814.9(3)
<i>Z</i>	2	4	4
<i>D</i> <sub>calc</sub> (g cm <sup>-3</sup> )	2.596	2.638	2.476
<i>T</i> (K)	90(2)	90(2)	90(2)
$\mu$ (cm <sup>-1</sup> )	30.51	33.14	30.40
<i>R</i> 1 <sup>a</sup>	0.0311	0.0268	0.0496
w <i>R</i> 2 <sup>b</sup>	0.0845	0.0539	0.0903

$$^a R1 = \sum(|F_o| - |F_c|) / \sum |F_o|.$$

$$^b wR2 = [\sum(w(F_o^2 - F_c^2)^2) / \sum(wF_o^2)]^{1/2}.$$

reaction of Zn(NO<sub>3</sub>)<sub>2</sub>·6H<sub>2</sub>O, MoO<sub>3</sub>, pca and H<sub>2</sub>O in the mole ratio 2.5:2:1:2000 at 180°C yielded ZnMoO<sub>4</sub> and a mixture of amorphous materials.

The infrared spectra of **1** and **2** exhibit a medium intensity band in the 3200–3300 cm<sup>-1</sup> range attributed to  $\nu(\text{N-H})$  of the pca ligand, which is not present in the spectrum of **3**, as expected. Additional ligand bands for the pca of **1** and **2** are found at ca. 1655, 1575 and 1285 cm<sup>-1</sup>. The strong bands in the 840–960 cm<sup>-1</sup> range of **1** and **2** are attributed to  $\nu(\text{Mo=O})$  and  $\nu(\text{Mo-O-Mo})$ .

### Crystal Structures

As shown in Fig. 1, the structure of  $[\{\text{Ni}(\text{pca})(\text{H}_2\text{O})\}_2\text{Mo}_8\text{O}_{26}]\cdot 2\text{H}_2\text{O}$  ( $1\cdot 2\text{H}_2\text{O}$ ) consists of discrete molecular clusters and isolated water molecules of

crystallization. The cluster consists of an octamolybdate unit  $\{\text{Mo}_8\text{O}_{26}\}^{4-}$  in the well-documented  $\beta$ -form (18), decorated with two  $\{\text{Ni}(\text{pca})(\text{H}_2\text{O})\}^{2+}$  subunits, each linked to the cluster through molybdenyl groups (Mo=O) of adjacent  $\{\text{MoO}_6\}$  octahedra. While five isomers of  $\{\text{Mo}_8\text{O}_{26}\}^{4-}$  have been described (7, 19), the  $\beta$ -form is the most compact, constructed exclusively of  $\{\text{MoO}_6\}$  octahedra in an efficient edge-sharing assembly. The Ni(II) sites exhibit distorted  $\{\text{NiO}_3\text{N}_3\}$  octahedral geometry through coordination to the three nitrogen donors of the pca ligand, two oxo-groups from the  $\beta$ - $\{\text{Mo}_8\text{O}_{26}\}^{4-}$  cluster and an aqua ligand. The pca nitrogen donors adopt a *facial* configuration about the Ni center.

Structures constructed from octamolybdate clusters decorated with peripheral  $\{M(\text{ligand})\}^{+n}$  moieties have been described previously, for example in the cases of

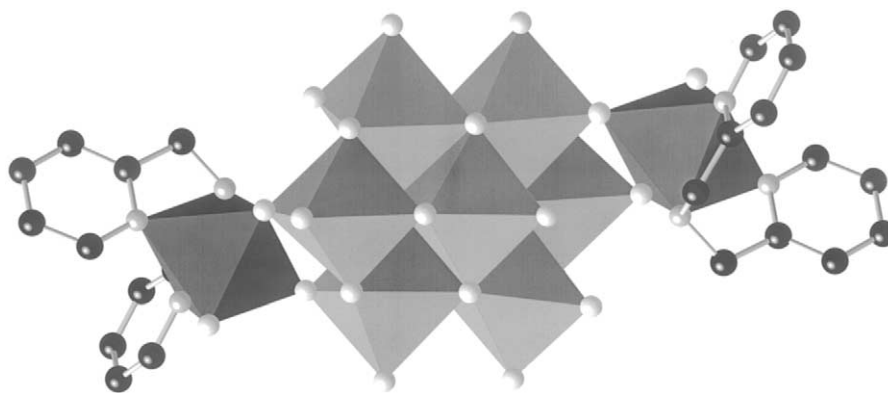


**FIG. 1.** A polyhedral representation of the structure of  $[\{\text{Ni}(\text{pca})(\text{H}_2\text{O})\}_2\text{Mo}_8\text{O}_{26}]$  (**1**).

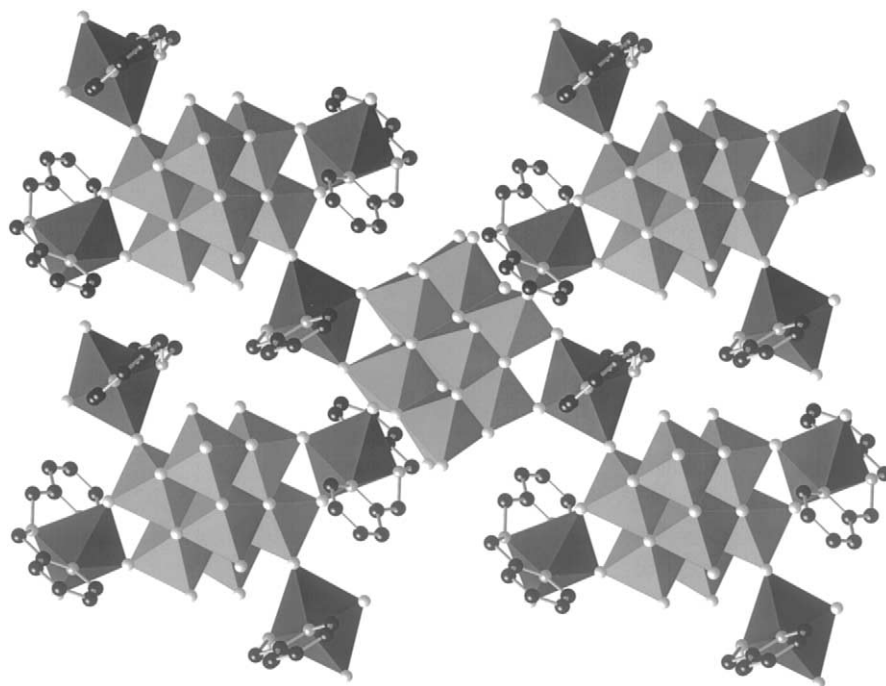


FIG. 2. A view of the network structure of  $[\{\text{Cu}(\text{pca})\}_2\text{Mo}_8\text{O}_{26}]$  (**2**).

$[\{\text{Cu}(\text{o-phen})_2\}_2\text{Mo}_8\text{O}_{26}]$  (**19**) and  $[\{\text{Cu}(\text{en})_2\}_2\text{Mo}_8\text{O}_{26}]$  (**20**). It is noteworthy that the  $\{\text{Mo}_8\text{O}_{26}\}^{4-}$  subunits of these materials adopt the  $\alpha$ - and  $\delta$ -forms, respectively. The five isomeric forms of octamolybdate are interrelated by minimal bond breaking through lengthening of weak axial interactions and rotations of the polyhedra. Since there are relatively small energy differences between these structural types, the occurrence of a particular isomer in the hydrothermal product is not predictable.

The structure of **1** is also distinct from those of other examples of molybdenum oxides incorporating  $\{\text{Ni}(\text{II})(\text{ligand})\}^{+n}$  subunits. Thus,  $[\{\text{Ni}(2,2'\text{-bpy})_2\}_2\text{Mo}_4\text{O}_{14}]$  (**21**) consists of a simple ring structure of two  $\{\text{Mo}_2\text{O}_7\}^{2-}$  units linked by two  $\{\text{Ni}(\text{bpy})_2\}^{2+}$  groups into a cluster with a  $\{\text{Mo}_4\text{Ni}_2\text{O}_6\}$  ring core. On the other hand,  $[\text{Ni}(2,2'\text{-bpy})_2\text{Mo}_4\text{O}_{13}]$  (**22**) is constructed from  $\beta$ - $\{\text{Mo}_8\text{O}_{26}\}^{4-}$  clusters linked through  $\{\text{Ni}(\text{bpy})_2\}^{2+}$  units into a one-dimensional chain. However, the molecular structure of **1** persists under a variety of conditions and cannot be induced to rearrange into one- or two-dimensional architectures.

As shown in Fig. 2, the structure of  $[\{\text{Cu}(\text{pca})\}_2\text{Mo}_8\text{O}_{26}]$  (**2**) is a two-dimensional network, constructed from  $\beta$ - $\{\text{Mo}_8\text{O}_{26}\}^{4-}$  clusters, linked through  $\{\text{Cu}(\text{pca})\}^{2+}$  subunits. Each molybdate cluster is linked through six (Mo=O) molybdenyl oxo-groups to four  $\{\text{CuN}_3\text{O}_3\}$  subunits, which bridge to four adjacent  $\beta$ - $[\text{Mo}_8\text{O}_{26}]^{4-}$  clusters. The Cu(II) sites adopt the common Jahn–Teller distorted “4 + 2” coordination mode, with the three nitro-

gen donors of the pca ligand and a short Cu–O bond (1.965(2) Å) defining the plane, and two long Cu–O bonds (2.340(2) and 2.490(2) Å) in the axial positions. In contrast to the *facial* disposition of pca nitrogen donors in **1**, the nitrogen donors of the ligand adopt a *meridional* configuration about the Cu site of **2**. This coordination mode orients the pyridyl rings approximately normal to the  $\{\text{CuMo}_4\text{O}_{13}\}$  bimetallic oxide plane. The metal–oxygen connectivity pattern produces 24-membered  $\{\text{Cu}_4\text{Mo}_8\text{O}_{12}\}$  rings. The amine nitrogens of the ligand are directed into the ring-cavity. The amine nitrogen exhibits hydrogen bonding to a molybdenyl oxo-group of an adjacent cluster with an  $\text{N}\cdots\text{O}$  of 2.83(1) Å,  $\text{H}\cdots\text{O}$  of 1.87(1) Å and an angle  $\text{O}\cdots\text{H}-\text{N}$  of ca. 178°.

Several structures constructed from octamolybdate clusters and Cu(II)-organoimine subunits have been described previously. These include  $[\{\text{Cu}_2(\text{tpypz})(\text{H}_2\text{O})_2\}\text{Mo}_8\text{O}_{26}]$  (tpypz = tetrapyridylpyrazine) (**23**) and  $[\{\text{Cu}_3(4,7\text{-phen})_3\}_2\text{Mo}_{14}\text{O}_{45}]$  (**24**), which exhibit  $\alpha$ - and  $\beta$ - $\{\text{Mo}_8\text{O}_{26}\}^{4-}$  building blocks, respectively. Curiously, the use of the tridentate ligand terpyridine (terpy) results in the isolation of  $[\text{Cu}(\text{terpy})\text{Mo}_2\text{O}_7]$  (**25**), a one-dimensional chain constructed from tetranuclear  $\{\text{Mo}_4\text{O}_{14}\}^{4-}$  clusters bridged by  $\{\text{Cu}(\text{terpy})\}^{2+}$  units. In this case, the Cu(II) site exhibits “4 + 1” square pyramidal geometry.

The structure of  $[\{\text{Cu}_3(\text{pca})_3\text{MoO}_4\}\text{Mo}_8\text{O}_{26}]\cdot 2\text{H}_2\text{O}$  (**3**·2H<sub>2</sub>O), shown in Fig. 3, consists of one-dimensional chains with water molecules of crystallization occupying interchain sites. The chains are constructed from

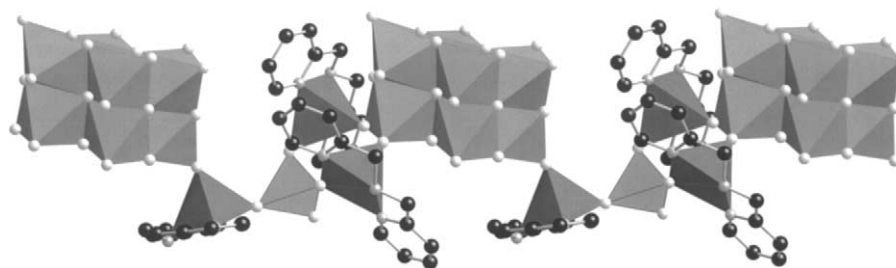


FIG. 3. A view of the one-dimensional structure of  $[\text{Cu}_3(\text{pca})_3\text{MoO}_4]\text{Mo}_8\text{O}_{26}$  (**3**).

$\beta\text{-}\{\text{Mo}_8\text{O}_{26}\}^{4-}$  clusters linked through unique  $\{\text{Cu}_3(\text{pca})_3\text{MoO}_4\}^{4+}$  subunits. These latter structural components consist of a tetrahedral  $\{\text{MoO}_4\}$  core tethered through bridging oxo-groups to three  $\{\text{Cu}(\text{pca})\}^{2+}$  moieties. The Cu(II) sites exhibit square pyramidal “4 + 1” coordination geometries, with the basal plane defined by two pyridyl nitrogen and an amine nitrogen donors from the tridentate pca ligand and a bridging oxo-group from the tetrahedral  $\{\text{MoO}_4\}^{2-}$  site, and with the apical position occupied by a bridging oxo-group from the  $\beta\text{-}\{\text{Mo}_8\text{O}_{26}\}^{4-}$  cluster. As expected, the  $\text{Cu}\text{-O}_{\text{basal}}$  bond distance (1.912(4) Å, ave.) is considerably shorter than the  $\text{Cu}\text{-O}_{\text{apical}}$  bond length (2.417(5) Å, ave.). Each octamolybdate subunit is linked to two  $\{\text{Cu}_3(\text{pca})_3\text{MoO}_4\}^{4+}$  building blocks, through two molybdenyl groups ( $\text{Mo}=\text{O}_{\text{terminal}}$ ) at one end and through a single molybdenyl group at the other terminus. Each  $\{\text{Cu}_3(\text{pca})_3\text{MoO}_4\}^{4+}$  subunit in turn bridges two  $\beta\text{-}\{\text{Mo}_8\text{O}_{26}\}^{4-}$  clusters of the chain.

The pyridyl groups of the pca ligands project outward from the bimetallic oxide chain and interdigitate with pyridyl groups from neighboring chains. The hydrogen atoms of the amine nitrogens of the pca ligands also project into the interchain space and exhibit weak hydrogen bonding to the oxo-groups of neighboring chains ( $\text{N}\cdots\text{O}$ , 2.89 Å).

#### Thermal Behavior

The thermal decomposition of  $\mathbf{1}\cdot 2\text{H}_2\text{O}$  exhibits weight loss of ca. 2.0% between 120 and 135°C, corresponding to the loss of the water molecules of crystallization (theoretical: 2.03%). This dehydration process is followed by a weight loss of ca. 1.0% at 220–240°C, attributed to the loss of the aqua ligand associated with the Ni(II) site of the compound. Since the mechanism of dehydration is dependent on energetic and topological considerations, the higher temperature of dehydration for the coordinated water molecule with respect to the water of crystallization is not anticipated. A final weight loss of ca. 20% occurs in the temperature range 290–360°C, due to ligand decomposition. The greenish-gray residue analyzes for  $\text{NiMoO}_4$  and  $\text{MoO}_3$ .

The TGA of **2** is characterized by weight losses of ca. 10 and 12% in the ranges 260–320°C and 350–420°C, respec-

tively, from the two-step decomposition of the pca ligand. The residue is an amorphous gray material. The thermal behavior of  $\mathbf{3}\cdot 2\text{H}_2\text{O}$  is characterized by a weight loss of ca. 2.0%, between 80 and 110°C, attributed to the loss of water of crystallization (theoretical: 1.67%). This dehydration process is followed by a weight loss of ca. 28–30% in the range 275–400°C, to give an amorphous blue-gray material (theoretical weight loss for the pca ligands: 27.5%).

#### CONCLUSIONS

The isolation of compounds **1** and **2** illustrates the observation that small amounts of organic components may profoundly influence the structures of metal oxide phases. The organic ligand through coordination to the metal adopts a dual role: it prevents the formation of dense-phase materials and structurally simple oxides and it serves to stabilize the observed architectures. It is also apparent that the coordination preferences of the secondary metal center are significant structural determinants, which may dictate even the dimensionality of the bimetallic oxide substructure.

#### ACKNOWLEDGMENTS

This work was supported by NSF grant CHE9987471.

#### REFERENCES

1. D. Hagrman, P. Hagrman, and J. Zubieta, *Angew. Chem., Int. Ed. Engl.* **38**, 3165 (1999).
2. P. B. Venuto, *Microporous Mater.* **2**, 297 (1994).
3. C. T. Kresge, M. E. Leonowicz, W. J. Roth, J. C. Vartuli, and J. S. Beck, *Nature* **359**, 710 (1992).
4. A. K. Cheetham, G. Férey, and T. Loiseau, *Angew. Chem. Int. Ed. Engl.* **38**, 3268 (1999).
5. D. B. Mitzi, *Prog. Inorg. Chem.* **48**, 1 (1999).
6. P. J. Hagrman and J. Zubieta, *Inorg. Chem.* **40**, 2800 (2001).
7. P. J. Hagrman, D. Hagrman, and J. Zubieta, *Angew. Chem. Int. Ed. Engl.* **38**, 2638 (1998).
8. D. Hagrman and J. Zubieta, *C. R. Acad. Sci. Paris, Sér. IIC, Chimie* **3**, 231 (2000).
9. P. J. Zapf, C. J. Warren, R. C. Haushalter, and J. Zubieta, *Chem. Commun.* 1543 (1997).

10. P. J. Hagrman and J. Zubieta, *Inorg. Chem.* **39**, 5218 (2000).
11. R. Finn and J. Zubieta, *Chem. Commun.* 1321 (2000).
12. Siemens "SMART Software Reference Manual;" Siemens, ed. Siemens Analytical X-ray Instruments, Inc., Madison, WI, 1994.
13. G. M. Sheldrick, Ed., "SADABS: Program for Empirical Absorption Corrections." University of Gottingen, Germany, 1996.
14. G. M. Sheldrick, Ed., "SHELXL96. Program for the Refinement of Crystal Structures." University of Gottingen, Germany, 1996.
15. J. Gopalakrishnan, *Chem. Mater.* **7**, 1265 (1995).
16. R. Faure, H. Loiseleur, and G. Thomas-David, *Acta Crystallogr. Sect. B* **29**, 1890 (1973).
17. (a) C. Pelizzi and G. Pelizzi, *Trans. Met. Chem.* **6**, 315 (1981); (b) L.-L. Zi, Y.-Z. Zhou, S.-J. Tu, S.-C. Liu, and X.-L. Jin, *Chin. J. Struct. Chem. (Tiegou Huaxue)* **16**, 379 (1997).
18. M. T. Pope, "Heteropoly and Isopoly Oxometalates," Springer, New York, 1983.
19. D. Hagrman, P. J. Hagrman, and J. Zubieta, *Comments Inorg. Chem.* **21**, 225 (1999).
20. J. R. D. DeBord, R. C. Haushalter, L. M. Meyer, D. J. Rose, P. J. Zapf, and J. Zubieta *Inorg. Chim. Acta* **256**, 165 (1997).
21. Y. Zhang, P. J. Zapf, L. M. Meyer, R. C. Haushalter, and J. Zubieta, *Inorg. Chem.* **36**, 2159 (1997).
22. P. J. Zapf, C. J. Warren, R. C. Haushalter, and J. Zubieta, *Chem. Commun.*, 1543 (1997).
23. D. Hagrman, P. Hagrman, and J. Zubieta, *Inorg. Chem. Acta* **300-302**, 212 (2000).
24. D. Hagrman, P. J. Zapf, and J. Zubieta, *Chem. Commun.* 1283 (1998).
25. P. J. Hagrman and J. Zubieta *Inorg. Chem.* **39**, 5218 (2000).